


TECHNICAL REPORT

Open Access



Survey of conditions for artificial aurora experiments at EISCAT Tromsø using dynasonde data

T. T. Tsuda^{1*} , M. T. Rietveld^{2,3}, M. J. Kosch^{4,5,6}, S. Oyama^{7,8}, K. Hosokawa¹, S. Nozawa⁷, T. Kawabata⁷, A. Mizuno⁷ and Y. Ogawa^{8,9}

Abstract

We report a brief survey on conditions for artificial aurora optical experiments in *F* region heating with O-mode at the EISCAT Tromsø site using dynasonde data from 2000 to 2017. The results obtained in our survey indicate the following: The possible conditions for conducting artificial aurora experiments are concentrated in twilight hours in both evening and morning, compared with late-night hours; the possible conditions appear in fall, winter, and spring, while there is no chance in summer, and the month-to-month variation among fall, winter, and spring is not clear. The year-to-year variation is well correlated with the solar cycle, and experiments during the solar minimum would be almost hopeless. These findings are useful for planning future artificial aurora optical experiments.

Keywords: Artificial aurora, Ionospheric heating, EISCAT, Tromsø, Dynasonde

Background

Many researchers have been working on ionospheric heating experiments using high frequency (HF) radio waves to understand phenomenon such as the interaction processes between radio waves and plasma particles, which is an essential part of plasma physics. A detailed overview on ionospheric heating experiments can be found in Kosch et al. (2007), Leyser and Wong (2009). There are several types of ionospheric heating experiments, but here we focus on artificial aurora experiments using *F* region heating with the ordinary mode (O-mode) at the European Incoherent SCATter (EISCAT) heating facility (Rietveld et al. 1993, 2016), to assist in the planning of such experiments in the future.

The EISCAT heating facility is one of several powerful tools for such ionospheric heating experiments, which is a high-power HF transmitter system at the EISCAT Tromsø site (69.6°N, 19.2°E). Using the EISCAT heating system, many researchers have performed *F* region

heating experiments with O-mode polarization during nighttime to detect optical emissions in artificial auroras (e.g., Gustavsson et al. 2005; Bryers et al. 2013; Kosch et al. 2014a, b; Blagoveshchenskaya et al. 2014). These published papers are obviously based on successful heating experiments. On the other hand, a large number of experiments might not have been successful, and they were never published.

A main cause of such unsuccessful experiments would be due to the ionospheric condition, which is not under the control of researchers. Note that another important factor would be the weather condition that limits optical observations, but we do not consider weather conditions in the present study for simplicity. To be more precise, O-mode heating can only be induced at a condition where the radio frequency of transmitted HF waves is slightly lower than the maximum plasma frequency in the heating region. Hence, if the radio frequency is higher than the *F* region critical frequency in O-mode heating (f_oF_2), the HF waves cannot induce any plasma resonance in the ionosphere. In the case of the EISCAT heating system, the minimum radio frequency is ~ 4 MHz. Then, f_oF_2 of at least 4 MHz during nighttime is needed for successful artificial aurora experiments.

*Correspondence: takuo.tsuda@uec.ac.jp

¹ Department of Computer and Network Engineering, The University of Electro-Communications (UEC), Chofu, Japan

Full list of author information is available at the end of the article

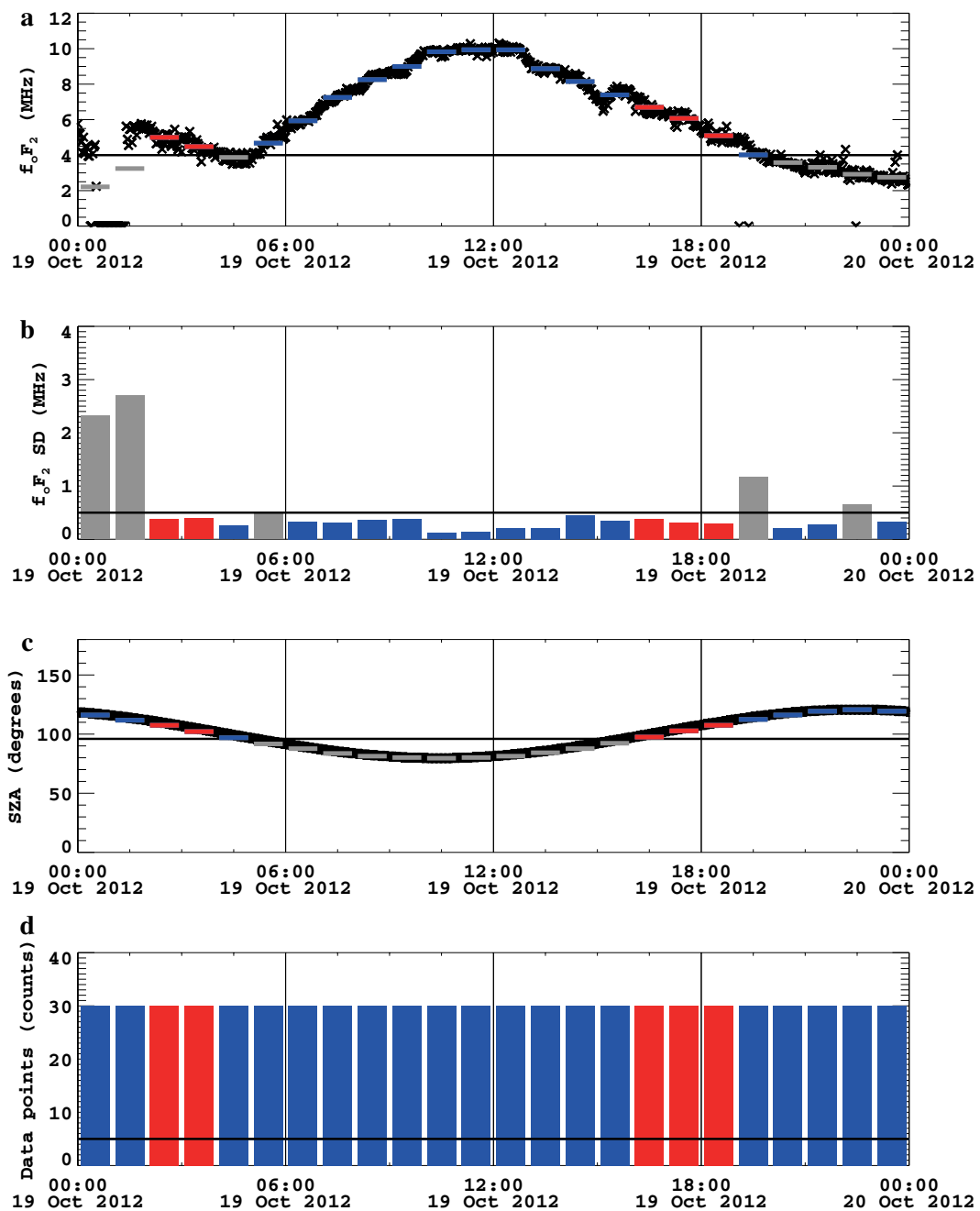


Fig. 1 **a** Variation in f_oF_2 on October 19, 2012. The black horizontal line corresponds to the threshold, i.e., 4 MHz. The shorter horizontal lines represent the averaged values for each hour. **b** Variation in one standard deviation (SD) of f_oF_2 for each hour. The black horizontal line corresponds to the threshold, i.e., 0.5 MHz. **c** Variation in the solar zenith angle (SZA). The black horizontal line corresponds to the threshold, i.e., 96°. The shorter horizontal lines represent the minimum values for each hour. **d** Variation in the number of f_oF_2 data for each hour. The black horizontal line corresponds to the threshold, i.e., 5. Each value, which satisfied each threshold, is shown in blue, otherwise in gray. When all the four thresholds were satisfied at the same time, the values at that time are marked in red. Note that the time is written in UT (= LT - 1 h (for winter time), at Tromsø)

Here, a vital question is when can such a condition be satisfied. There are many publications on f_oF_2 variation or F region electron density variation (e.g., Cai et al. 2007), and basic features of F region electron density

would be relatively well known, observationally as well as theoretically. However, this knowledge is not directly relevant to conditions for artificial aurora experiments because of missing information on the relationship

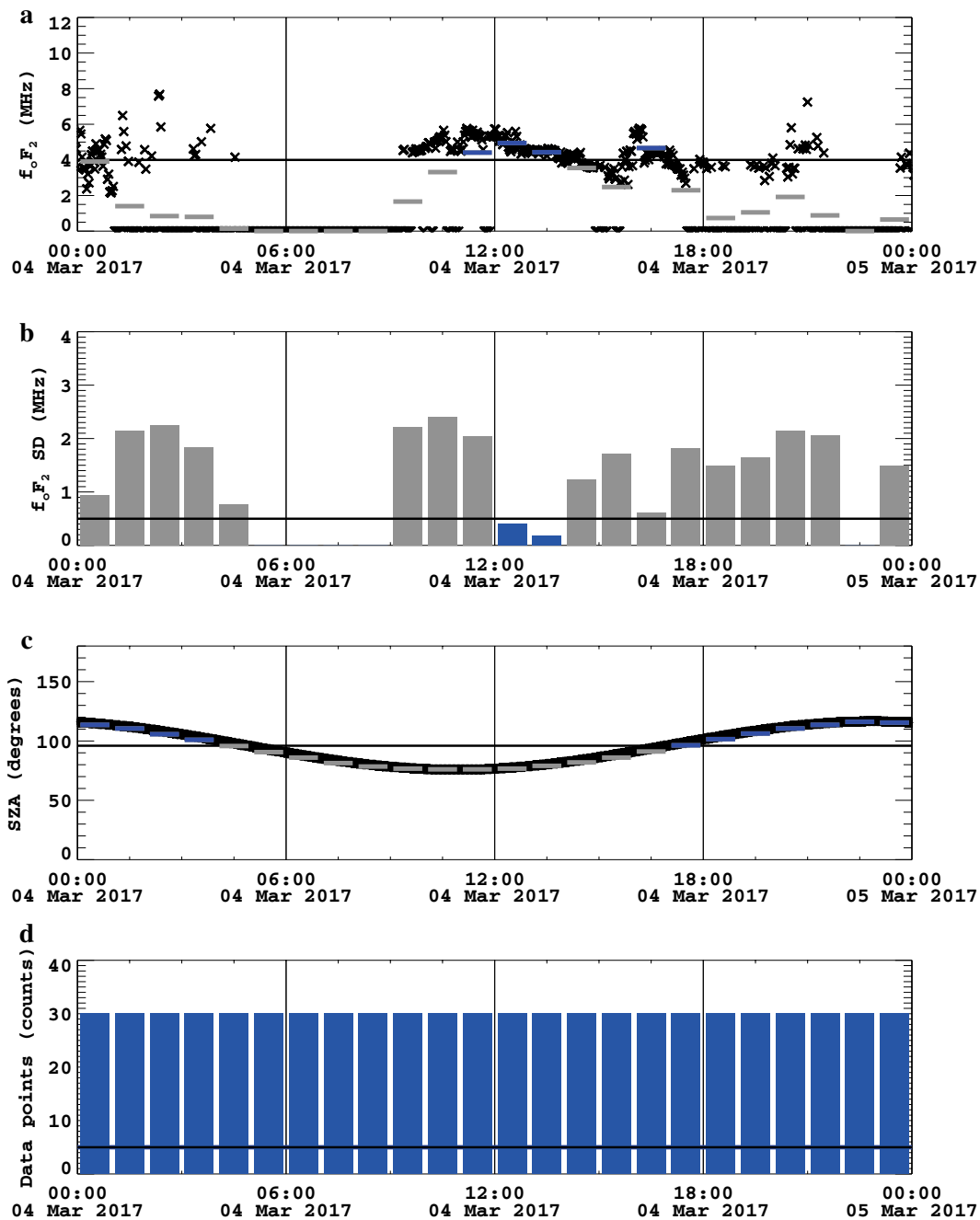


Fig. 2 Same as Fig. 1, but on March 4, 2017

between F region electron density (or f_oF_2) and nighttime hours [or solar zenith angle (SZA)], and it is not much useful to answer the question. Several researchers may be able to answer the question based on their valuable experience in such experiments. However, there is no investigation on this issue based on statistical data. To clarify this issue, in the present paper, we briefly report on our survey for artificial aurora experiments using a

statistical dataset obtained by the dynasonde (Rietveld et al. 2008) at the EISCAT Tromsø site.

Methods

For a statistical survey, we accumulated f_oF_2 data from 2000 to 2017 (precisely to 06:06 UT on October 11, 2017), obtained by the dynasonde at the EISCAT Tromsø site (69.6°N, 19.2°E). A sounding was made typically every

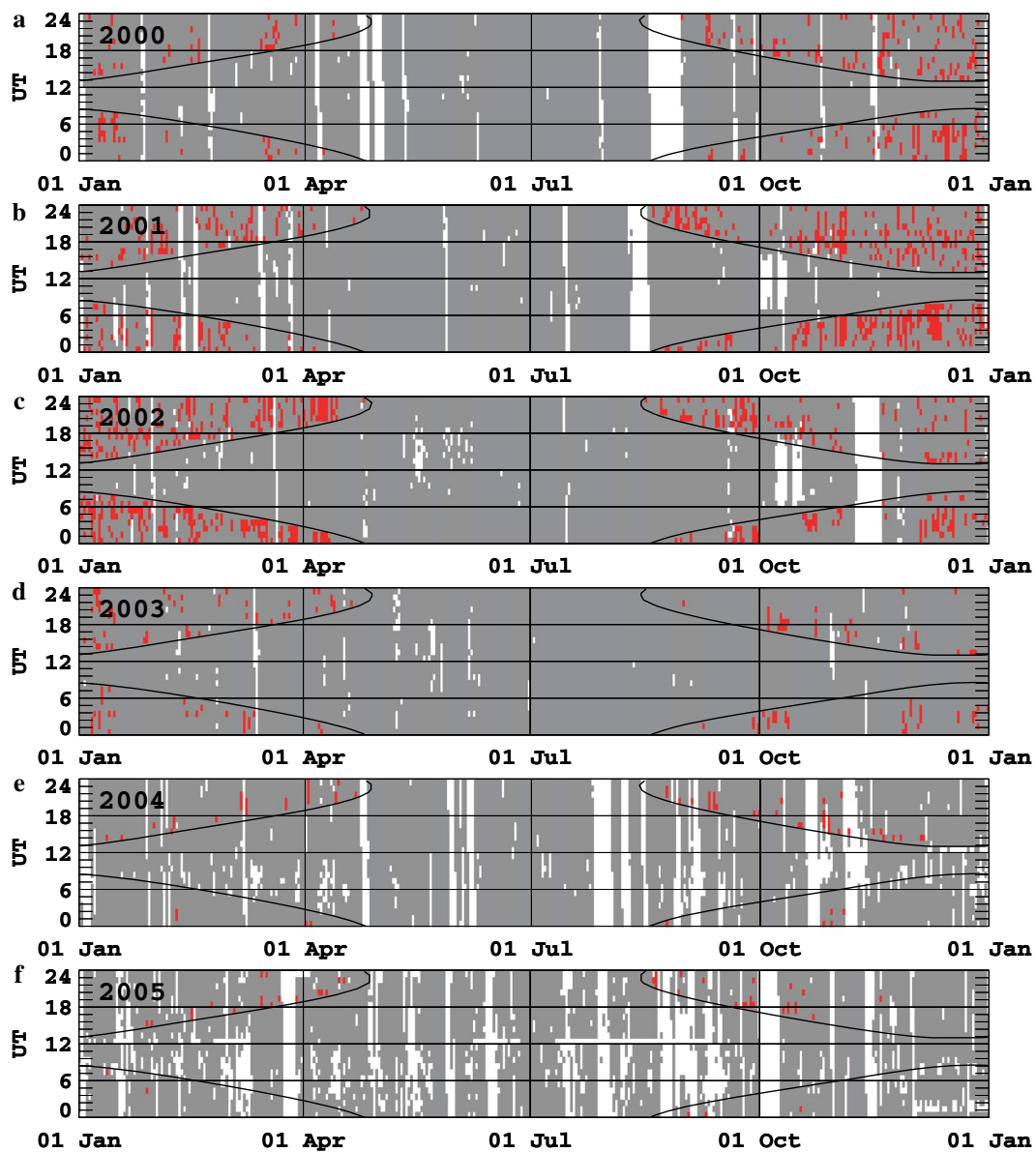


Fig. 3 Variations in possible UT-date for conducting artificial aurora experiments from 2000 to 2005 (from **a** to **f**). The red region indicates periods under the possible condition, and the gray region indicates periods under the impossible condition. The white region corresponds to periods when there are no data. The solar zenith angle (SZA) of 96° is described by the black curve. Note that $LT = UT + 1$ h (for winter time), at Tromsø

6 min before February 2012, and every 2 min since then. Using the dataset, we categorized the data of 1 h into three conditions: (a) possible nighttime heating condition; (b) impossible nighttime heating condition; and (c) no data. To judge the conditions, we set four criteria: (1) number of f_oF_2 data for each 1-h period is at least 5; (2) the averaged f_oF_2 for each 1-h period is more than or equal to 4 MHz; (3) one standard deviation of f_oF_2 for each 1-h period is less than or equal to 0.5 MHz; (4) the minimum solar zenith angle for each 1-h period is more than or equal to

96° . If criterion (1) is not satisfied, the data for each 1-h period are categorized under condition (c). If all criteria are satisfied, the data for each 1-h period are categorized under condition (a). Otherwise, the data of each 1-h period are categorized under condition (b). Note that criterion (2) is for O-mode heating, criterion (3) is for stable ionosphere or stable heating, which is important for ON-OFF heating operation, and criterion (4) is for nighttime, including both nautical twilight and astronomical twilight to detect optical emissions, i.e., artificial aurora emissions.

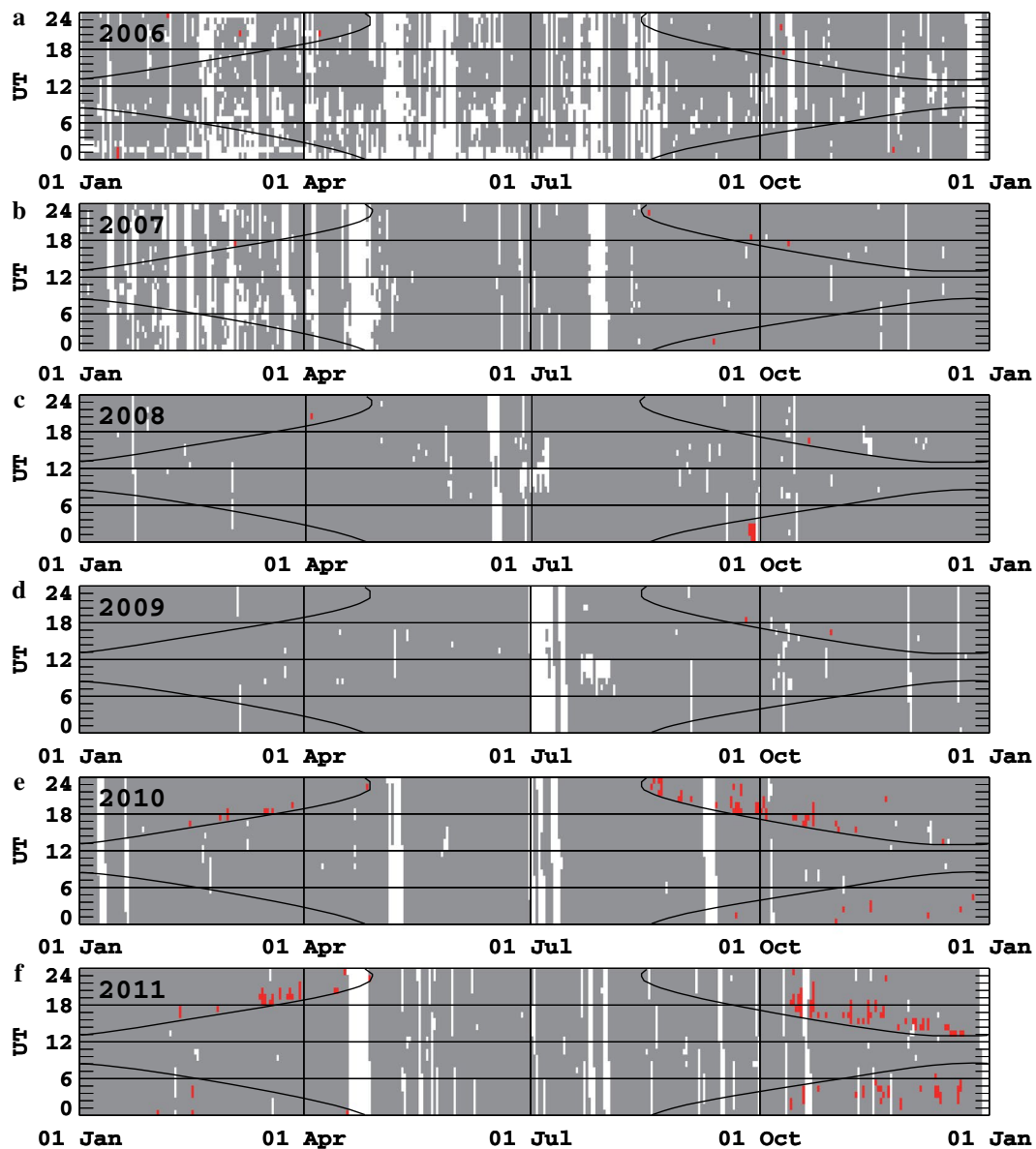


Fig. 4 Variations in possible UT-date for conducting artificial aurora experiments from 2006 to 2011 (from **a** to **f**). The red region indicates periods under the possible condition, and the gray region indicates periods under the impossible condition. The white region corresponds to periods when there are no data. The solar zenith angle (SZA) of 96° is described by the black curve. Note that $LT = UT + 1$ h (for winter time), at Tromsø

Results and discussion

Examples

Figure 1 shows the results obtained on October 19, 2012, as an example of possible nighttime heating condition. Note that this example corresponds to a day of successful experiment reported by Blagoveshchenskaya et al. (2014). The dynasonde was operated successively for 24 h, i.e., data were collected at intervals of 2 min, and the number of f_oF_2 dataset for each 1-h period was 30 (see Fig. 1d). At $\sim 12:00$ UT, f_oF_2 was ~ 10 MHz (see Fig. 1a), and the solar zenith angle was less than 90° (see Fig. 1c). This

means that the value of f_oF_2 in the sunlit time was sufficiently high for ionospheric heating (≥ 4 MHz). After that, the value of f_oF_2 decreased with increasing solar zenith angle. The solar zenith angle reached $\sim 96^\circ$ at $\sim 16:00$ UT, and criterion (4) was satisfied. Note that for a solar zenith angle of 96° , it was dark on the ground but sunlit in the F region. The values of f_oF_2 were still sufficiently high (≥ 4 MHz) at 16:00–20:00 UT, and standard deviations were sufficiently small (≤ 0.5 MHz) (see Fig. 1b), which satisfied criterion (3) at 16:00–19:00 UT. Hence, the data for 16:00–19:00 UT were categorized under condition (a),

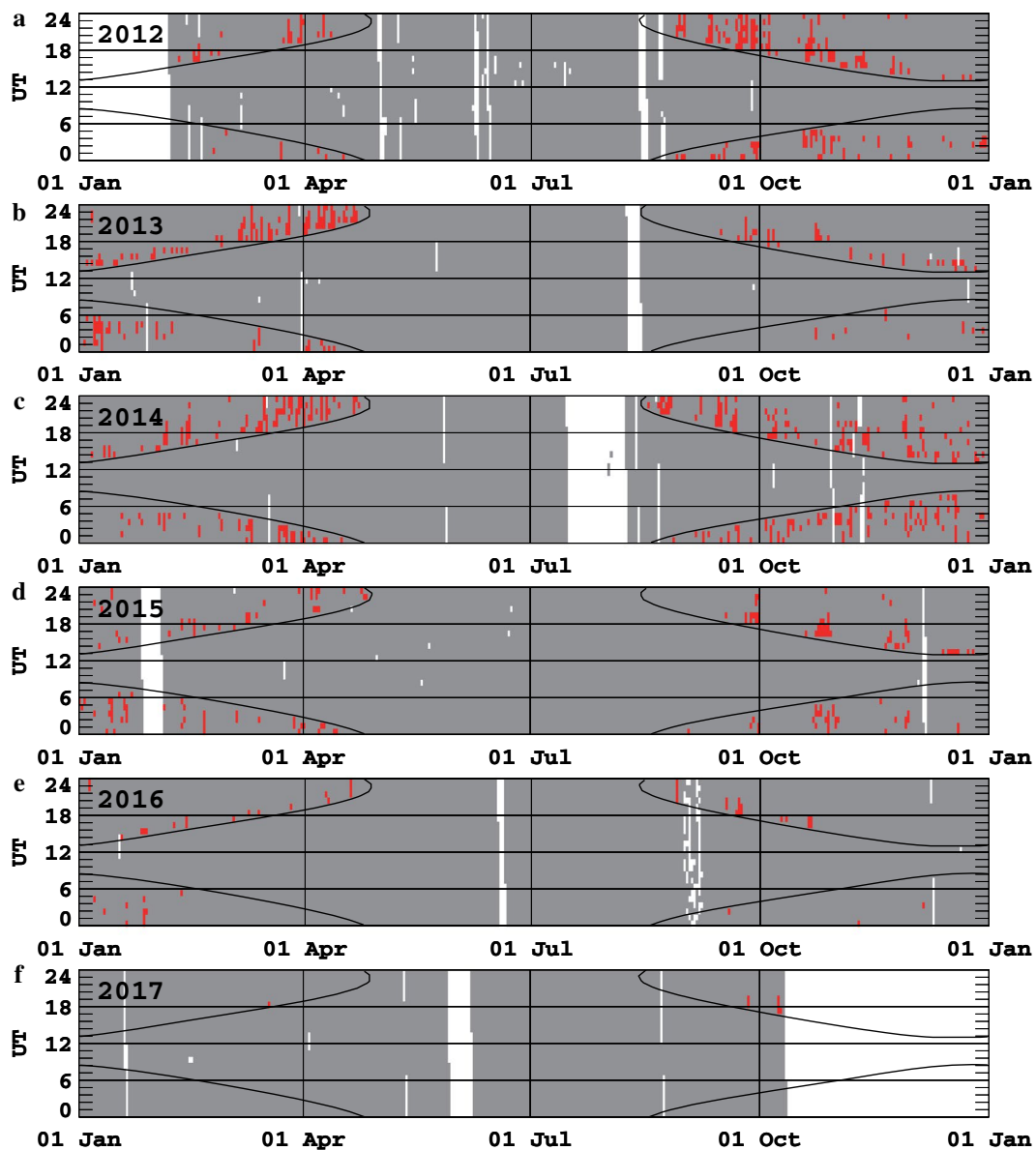


Fig. 5 Variations in possible UT-date for conducting artificial aurora experiments from 2012 to 2017 (from **a** to **f**). The red region indicates periods under the possible condition, and the gray region indicates periods under the impossible condition. The white region corresponds to periods when there are no data. The solar zenith angle (SZA) of 96° is described by the black curve. Note that $LT = UT + 1$ h (for winter time), at Tromsø

marked by red in Fig. 1. After 20:00 UT, the values of f_oF_2 were not sufficiently high (<4 MHz), and then, it does not satisfy the possible nighttime heating condition. Thus, if high electron density during daytime can be maintained for a few hours after sunset, we can observe possible nighttime heating condition in twilight hours. In addition, possible nighttime heating condition was observed in the morning from 02:00–04:00 UT. These high electron densities may be due to the transport of high electron density from dayside, e.g., owing to polar patches. Otherwise, it may be due to stable ionization by relatively

constant particle precipitation from the magnetosphere. In addition, ionization would contribute in the sunlit F region during twilight hours. Anyway, from the results, we found a few hours of possible nighttime heating condition on October 19, 2012, and it is consistent with the report by Blagoveshchenskaya et al. (2014).

Figure 2 shows the results obtained on March 4, 2017, as an example of the impossible nighttime heating condition. Note that this example corresponds to a day of our recent unsuccessful experiment, which has not been reported in any publications. As can be seen in the

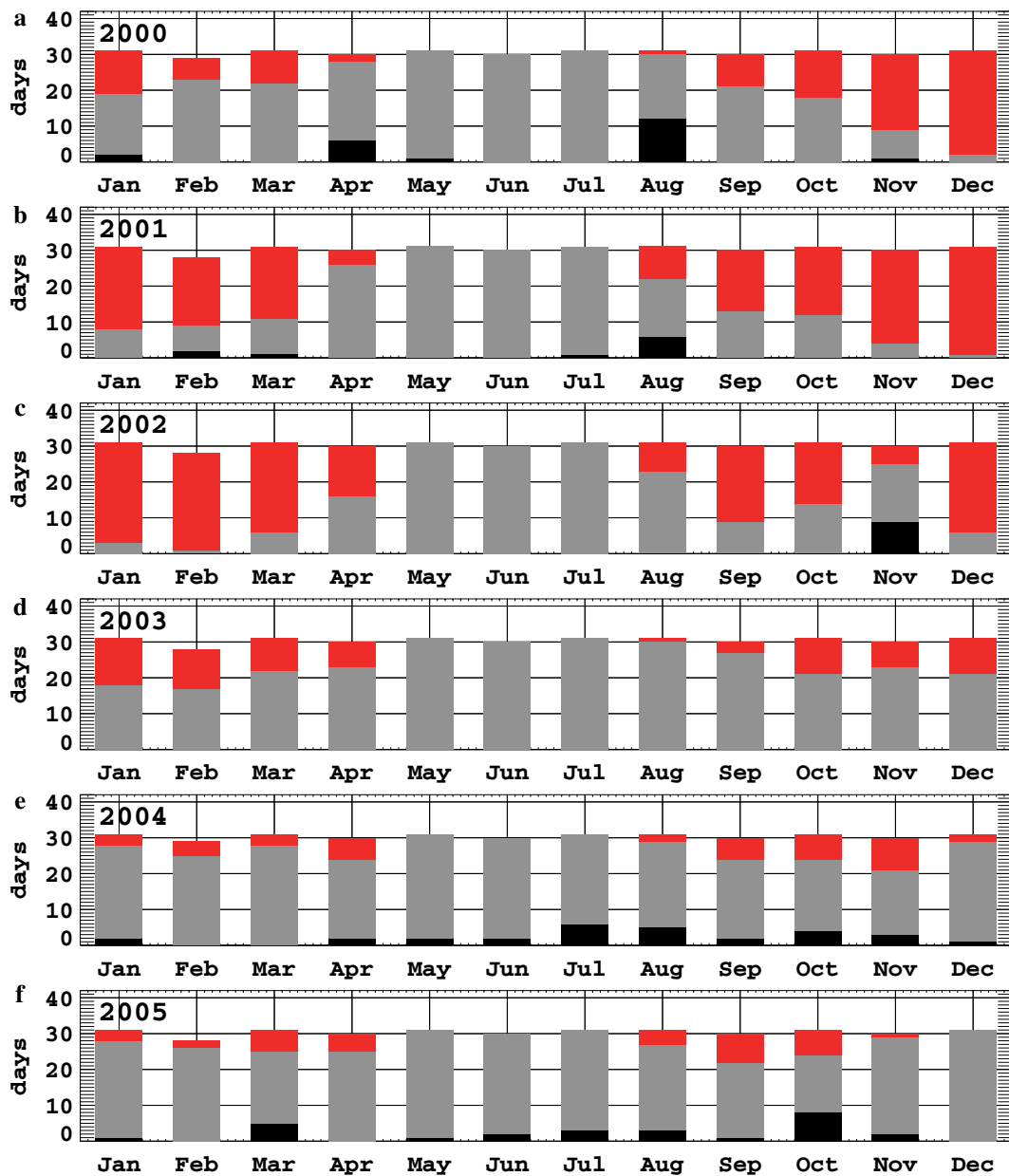


Fig. 6 Month-to-month variations of the number of possible days for conducting artificial aurora experiments from 2000 to 2005 (from **a** to **f**). The red bars indicate the possible days, while the gray bars indicate days in which conducting the experiments is not possible, and the black bars indicate days when there are no data

figure, f_oF_2 during daytime ($\sim 12:00$ UT) was not high (5–6 MHz) (see Fig. 2a), compared with the example on October 19, 2012. The value of f_oF_2 became smaller with increasing solar zenith angle, and then, it reached a value less than 4 MHz at 14:00–15:00 UT. After that, the solar zenith angle reached $\sim 96^\circ$ at $\sim 17:00$ UT (see Fig. 2c). Thus, it was not possible to conduct artificial aurora experiments in twilight hours. High values of f_oF_2

(≥ 4 MHz) were observed during nighttime, e.g., around 20:00–22:00 UT. However, these values were not sufficiently stable, i.e., one standard deviation was more than 0.5 MHz (see Fig. 2b). These high values of f_oF_2 would be probably due to unstable ionization by sporadic particle precipitation. We did not observe any possible nighttime heating condition on March 4, 2017, and it is consistent with our recent unsuccessful experiment.

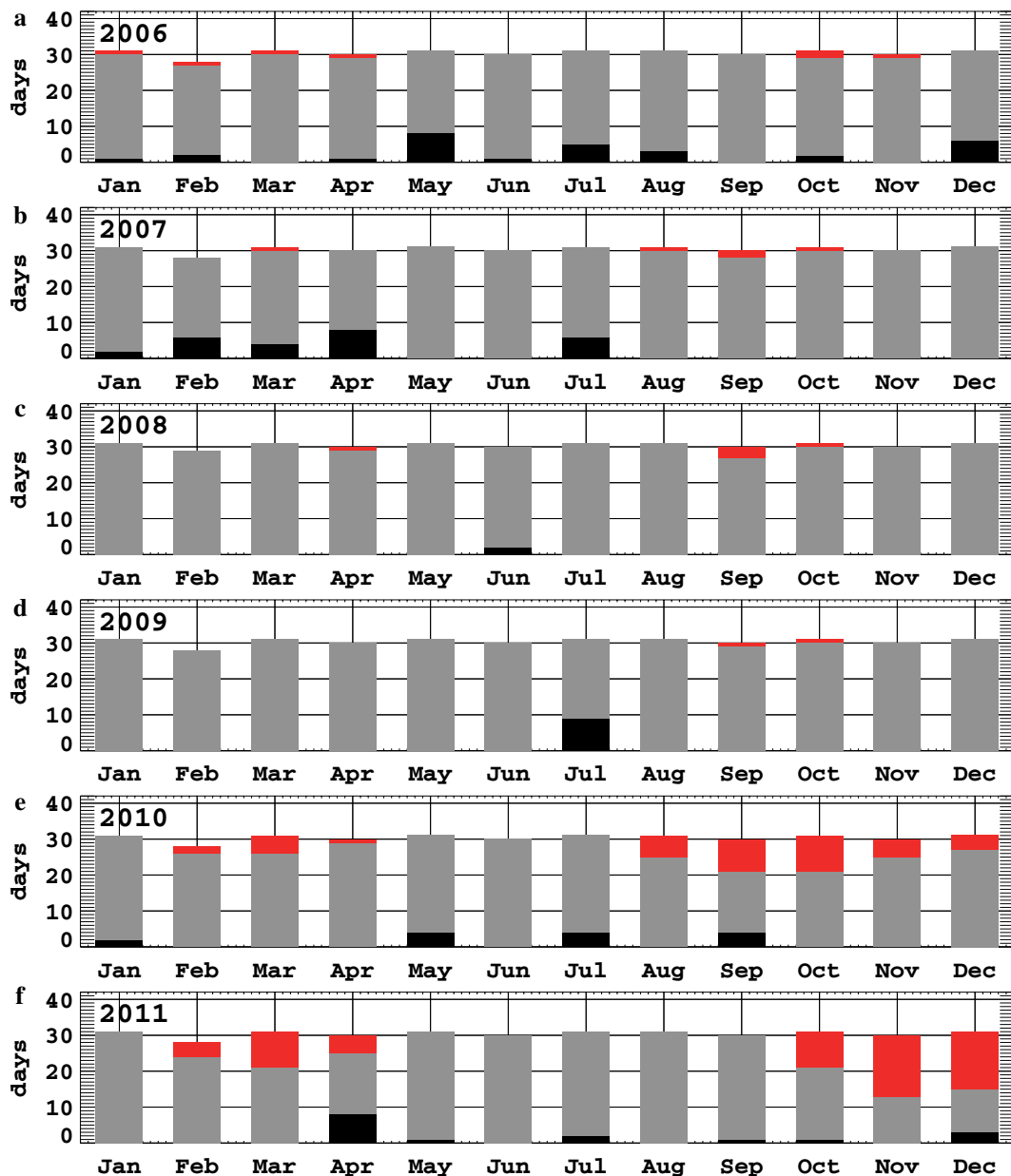


Fig. 7 Month-to-month variations of the number of possible days for conducting artificial aurora experiments from 2006 to 2011 (from **a** to **f**). The red bars indicate the possible days, while the gray bars indicate days in which conducting the experiments is not possible, and the black bars indicate days when there are no data

Local time variation

Figures 3, 4 and 5 shows UT-date variations for the possibility of conducting the artificial aurora experiments from 2000 to 2017. Obviously, no possible conditions were observed during summer, i.e., roughly May to July. This is because criterion (4) for nighttime condition is never satisfied during summer. It seems that possible hours of conducting artificial aurora experiments are fairly concentrated

around the evening hours, i.e., a few hours after sunset, compared with late-night hours. Another interesting characteristic is that a number of the possible hours were found in the morning, i.e., a few hours before sunrise. These indicate that a relatively high electron density can be maintained at twilight hours owing to solar illumination in the *F* region. In addition, there may be effects induced by the transport of high electron density from the dayside.

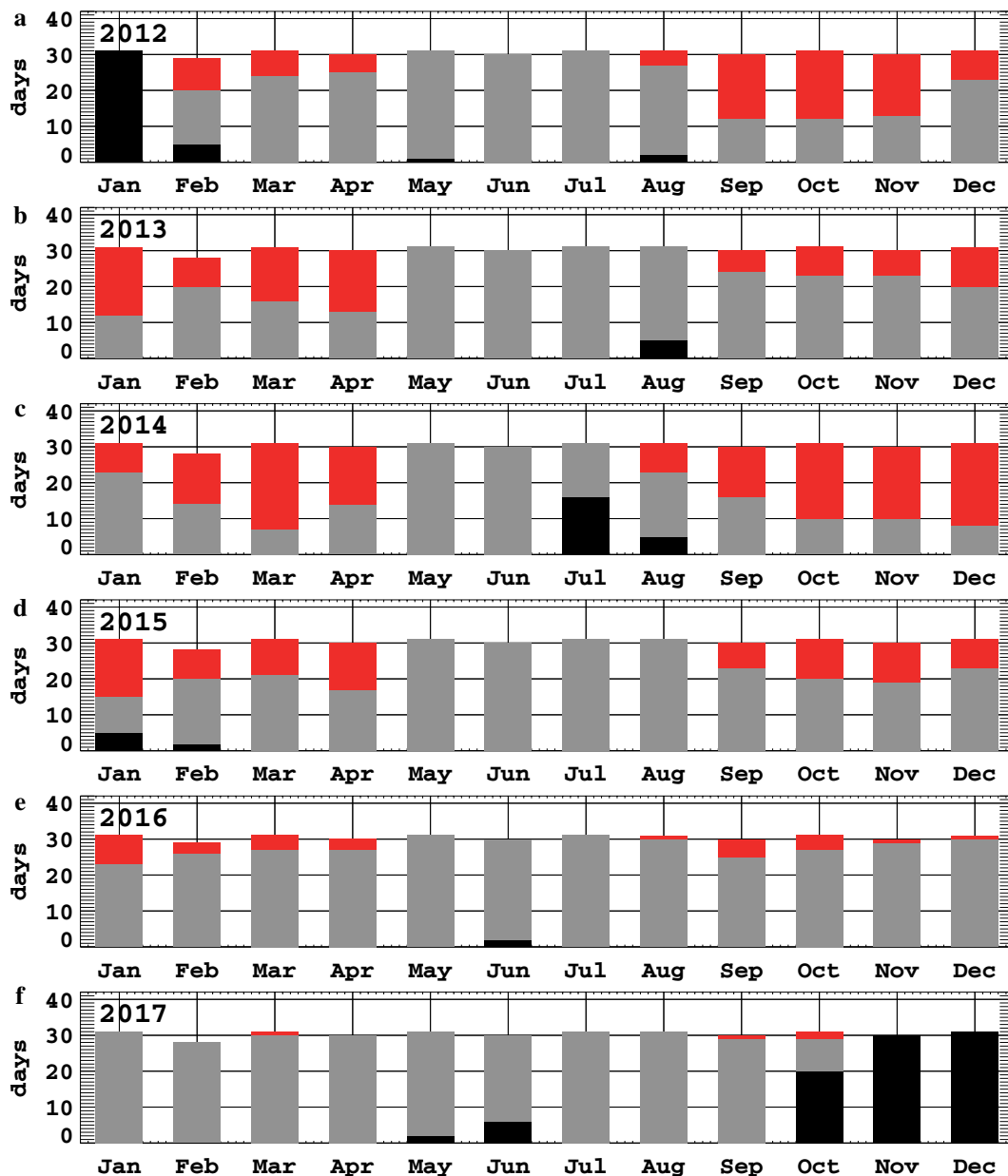
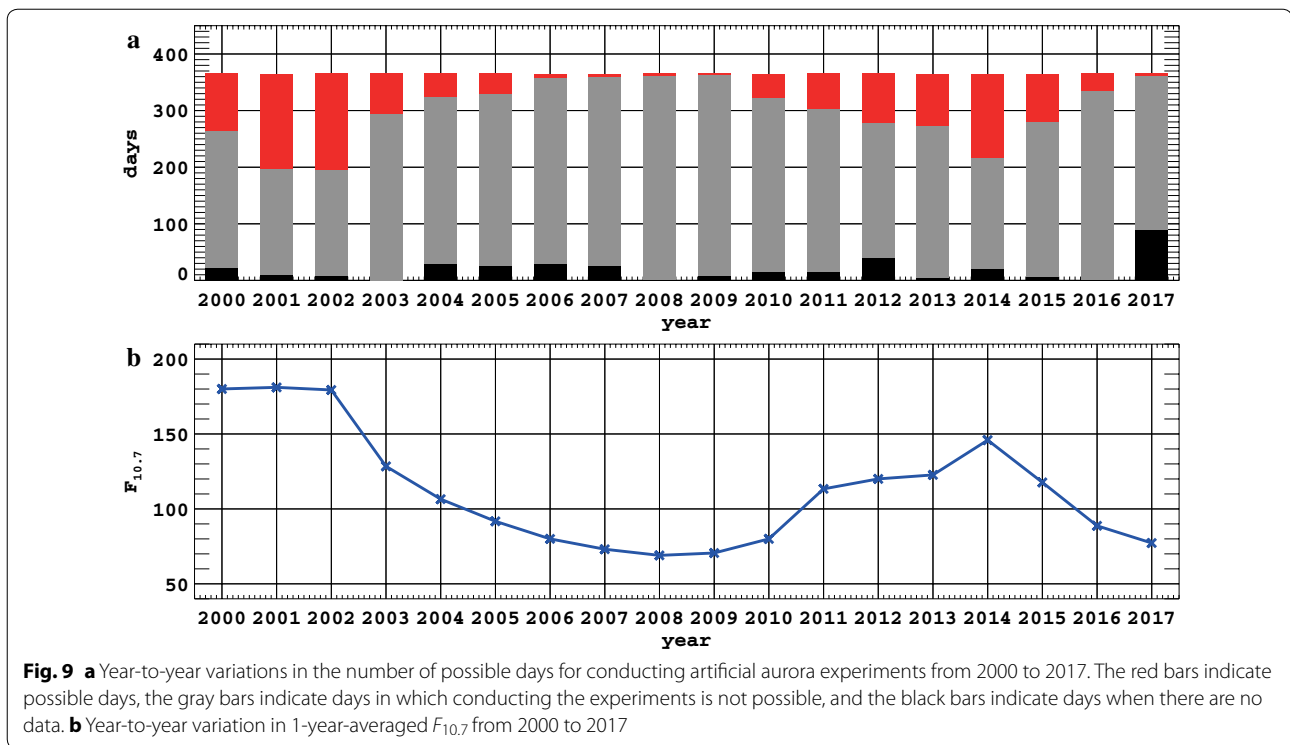


Fig. 8 Month-to-month variations of the number of possible days for conducting artificial aurora experiments from 2012 to 2017 (from a to f). The red bars indicate the possible days, while the gray bars indicate days in which conducting the experiments is not possible, and the black bars indicate days when there are no data

Seasonal variation

Figures 6, 7 and 8 shows the month-to-month variations of the number of possible days for conducting artificial aurora experiments from 2000 to 2017. Here, if there are no data in a day, we categorize the day under no data, marked by black. If there is at least 1 h in a day where it is possible to conduct experiments, we categorize the day under possible condition. Otherwise, we categorize the day under impossible condition. As mentioned above,

there was no possibility of conducting experiment from May to July, i.e., during summer. On the other hand, it was possible to conduct experiments from August to April, i.e., during the fall, winter, and spring seasons. Particularly, there were many possible days for conducting artificial aurora experiments in winter. It seems that the number of possible days during winter is similar to those during spring as well as fall. Generally, there should be differences in solar irradiation between winter and



spring/fall. Such seasonal differences would be mainly due to different solar zenith angles. However, in twilight hours, the solar zenith angle should be roughly constant in any season. Hence, a relatively high electron density can be maintained in the illuminated F region during the twilight hours in any season. This could be a reason for the observed unclear seasonal variation.

Year-to-year variation

Figure 9 shows year-to-year variations of the number of possible days for conducting artificial aurora experiments from 2000 to 2017, with a 1 year-average of the solar radio flux index at 10.7 cm (2,800 MHz), $F_{10.7}$. Note that the averaged $F_{10.7}$ in 2017 is calculated using data till August 31, 2017. We can find a clear relationship between the averaged $F_{10.7}$ and the number of possible days. For example, there were few possible days during 2007–2009 when the solar activity was low (the averaged $F_{10.7}$ was 70–80). The number of possible days had a small peak in 2014, and the solar activity also had a small peak in 2014 (the averaged $F_{10.7}$ was ~ 150). This indicates that the amount of solar flux, i.e., the solar activity, would be vitally important for the possibility to conduct artificial aurora experiments.

Conclusions

To investigate the possibility of conducting artificial aurora experiments based on statistical data, we

accumulated and analyzed the dynasonde data obtained from 2000 to 2017 at the EISCAT Tromsø site, which covers one solar cycle. From the results, we can obtain the following findings. Twilight hours in the evening and morning are possible for conducting artificial aurora experiments, compared with late-night hours. Possible conditions are observed in fall, winter, and spring seasons, while the summer season provides no possibility of conducting experiments, and the month-to-month variation among fall, winter, and spring seasons is not clear. The year-to-year variation is consistent with the solar cycle, and there is less possibility when the solar activity is low. According to the findings mentioned above, we suggest that the best periods for conducting artificial aurora experiments are the twilight hours in the evening and morning in the fall, winter, and spring seasons during the solar maximum. The next solar maximum, i.e., the maximum of cycle 25, would be 2022–2023 according to solar cycle predictions (e.g., Rigozo et al. 2011; Attia et al. 2013; Li et al. 2015). On the other hand, we do not recommend conducting experiments during the solar minimum. We believe that this information would be useful for planning future artificial aurora experiments.

Abbreviations

EISCAT: European Incoherent SCATter; HF: High frequency; LT: Local time; O-mode: Ordinary mode; SD: Standard deviation; SZA: Solar zenith angle; UT: Universal time.

Authors' contributions

TTT conducted data analysis and wrote the first draft of the manuscript. MTR accumulated the dataset by operating the dynasonde and supported the data analysis. MJK, SO, KH, SN, TK, AM, and YO contributed toward interpreting the results. All authors have contributed toward revising and improving the manuscript. All authors read and approved the final manuscript.

Author details

¹ Department of Computer and Network Engineering, The University of Electro-Communications (UEC), Chofu, Japan. ² European Incoherent SCATter (EISCAT) Scientific Association, Tromsø, Norway. ³ Department of Physics and Technology, University of Tromsø (UiT) - The Arctic University of Norway, Tromsø, Norway. ⁴ South African National Space Agency (SANSA), Hermanus, South Africa. ⁵ Department of Physics, Lancaster University, Lancaster, UK. ⁶ Department of Physics and Astronomy, University of the Western Cape, Bellville, South Africa. ⁷ Institute for Space-Earth Environmental Research (ISEE), Nagoya University, Nagoya, Japan. ⁸ National Institute of Polar Research (NIPR), Tachikawa, Japan. ⁹ Department of Polar Science, Graduate University for Advanced Studies (SOKENDAI), Tachikawa, Japan.

Acknowledgements

We thank European Incoherent SCATter (EISCAT) scientific association for providing dynasonde data. EISCAT is an international association supported by research organizations in China (CRIRP), Finland (SA), Japan (NIPR), Norway (NFR), Sweden (VR), and the United Kingdom (NERC). The dynasonde data can be available on request to M. T. Rietveld (mike@eiscat.uit.no) or can be accessed directly at the website, EISCAT Dynasonde (<http://dynserv.eiscat.uit.no/DD/login.php>). The 10.7 cm solar radio flux index data, $F_{10.7}$ data, are provided at the website, National Centers for Environmental Information (NCEI), National Oceanic and Atmospheric Administration (NOAA) (ftp://ftp.ngdc.noaa.gov/STP/GEOMAGNETIC_DATA/INDICES/KP_AP). This work was supported in part by MEXT/JSPS KAKENHI Grants, JP26610157, JP15H05747, JP15H05815, JP16H01171, JP16H02230, JP16H06021, JP16H06286, JP16K05569, and JP17H02968, by the Sumitomo Foundation Basic Science Research Grant, 150627, by National Institute of Polar Research (NIPR) through General Collaboration Project, 28-2, and by the joint research program of the Institute for Space-Earth Environmental Research (ISEE), Nagoya University.

Competing interests

The authors declare that they have no competing interests.

Ethics approval and consent to participate

Not applicable.

Publisher's Note

Springer Nature remains neutral with regard to jurisdictional claims in published maps and institutional affiliations.

Received: 5 November 2017 Accepted: 14 February 2018

Published online: 08 March 2018

References

- Attia AF, Ismail HA, Basurah HM (2013) A neuro-fuzzy modeling for prediction of solar cycles 24 and 25. *Astrophys Space Sci* 344:5–11. <https://doi.org/10.1007/s10509-012-1300-6>
- Blagoveshchenskaya NF, Borisova TD, Kosch M, Sergienko T, Brändström U, Yeoman TK, Häggström I (2014) Optical and ionospheric phenomena at EISCAT under continuous X-mode HF pumping. *J Geophys Res Space Phys* 119:10,483–10,498. <https://doi.org/10.1002/2014JA020658>
- Bryers CJ, Kosch MJ, Senior A, Rietveld MT, Singer W (2013) A comparison between resonant and nonresonant heating at EISCAT. *J Geophys Res Space Phys* 118:6766–6776. <https://doi.org/10.1002/jgra.50605>
- Cai HT, Ma SY, Fan Y, Liu YC, Schlegel K (2007) Climatological features of electron density in the polar ionosphere from long-term observations of EISCAT/ESR radar. *Ann Geophys* 25:2561–2569. <https://doi.org/10.5194/angeo-25-2561-2007>
- Gustavsson B, Sergienko T, Kosch MJ, Rietveld MT, Brändström BUE, Leyser TB, Isham B, Gallop P, Aso T, Ejiri M, Grydeland T, Steen Å, LaHoz C, Kaila K, Jussila J, Holma H (2005) The electron energy distribution during HF pumping, a picture painted with all colors. *Ann Geophys* 23:1747–1754. <https://doi.org/10.5194/angeo-23-1747-2005>
- Kosch MJ, Pedersen T, Rietveld MT, Gustavsson B, Grach SM, Hagfors T (2007) Artificial optical emissions in the high-latitude thermosphere induced by powerful radio waves: an observational review. *Adv Space Res* 40:365–376. <https://doi.org/10.1016/j.asr.2007.02.061>
- Kosch MJ, Vickers H, Ogawa Y, Senior A, Blagoveshchenskaya N (2014) First observation of the anomalous electric field in the topside ionosphere by ionospheric modification over EISCAT. *Geophys Res Lett* 41:7427–7435. <https://doi.org/10.1002/2014GL061679>
- Kosch MJ, Bryers C, Rietveld MT, Yeoman TK, Ogawa Y (2014) Aspect angle sensitivity of pump-induced optical emissions at EISCAT. *Earth Planets Space* 66:159. <https://doi.org/10.1186/s40623-014-0159-x>
- Leyser TB, Wong AY (2009) Powerful electromagnetic waves for active environmental research in geospace. *Rev Geophys* 47:RG1001. <https://doi.org/10.1029/2007RG000235>
- Li KJ, Feng W, Li FY (2015) Predicting the maximum amplitude of solar cycle 25 and its timing. *J Atmos Terr Phys* 135:72–76. <https://doi.org/10.1016/j.jastp.2015.09.010>
- Rietveld MT, Kohl H, Kopka H, Stubbe P (1993) Introduction to ionospheric heating at Tromsø - I. Experimental overview. *J Atmos Terr Phys* 55:577–599. [https://doi.org/10.1016/0021-9169\(93\)90007-L](https://doi.org/10.1016/0021-9169(93)90007-L)
- Rietveld MT, Wright JW, Zabolotn N, Pitteway MLV (2008) The Tromsø dynasonde. *Polar Sci* 2:55–71. <https://doi.org/10.1016/j.polar.2008.02.001>
- Rietveld MT, Senior A, Markkanen J, Westman A (2016) New capabilities of the upgraded EISCAT high-power HF facility. *Radio Sci* 51:1533–1546. <https://doi.org/10.1002/2016RS006093>
- Rigozo NR, Souza Echer MP, Evangelista H, Nordemann DJR, Echer E (2011) Prediction of sunspot number amplitude and solar cycle length for cycles 24 and 25. *J Atmos Terr Phys* 73:1294–1299. <https://doi.org/10.1016/j.jastp.2010.09.005>